Transported PDF modeling of turbulent premixed combustion

By Chong M. Cha

1. Motivation and objectives

Computational implementation of transported PDF methods for turbulent reacting flows (Pope 1985, 1990) use an ensemble of "notional" particles to represent the joint probability density function (PDF) of, most generally, the velocity, reacting scalars, and their dissipation rates. Following Pope (1997), the evolution equation for the i-th notional particle, among N_p total particles in an unresolved subdomain of the flow field, can be written as

$$\frac{d}{dt}\boldsymbol{\psi}^{(i)}(t) = (\mathcal{M} + \mathcal{S})\boldsymbol{\psi}^{(i)}, \tag{1.1}$$

where $\boldsymbol{\psi}$ represents a set of numbers defining the state space, $\mathcal{M}$ is the mixing or transport operator, and $\mathcal{S}$ is the source/sink operator. The operators map the state space onto itself. For simplicity, consider only the thermochemical state (a composition of N_s total species, the temperature or enthalpy, and pressure). Then $\boldsymbol{\psi}$ contains $N_s + 2$ elements. $\mathcal{S}$ is known *a priori* for a given chemical-kinetic scheme and heat-loss model (e.g. for radiation). For many practical engineering applications, these are highly nonlinear, but depend only on the single-point information of $\boldsymbol{\psi}$. $\mathcal{M}$, on the other hand, contains the spatial derivatives of $\boldsymbol{\psi}$ at scales below that of the subdomain and hence must be modeled. This is generally done with the available single-point information only, by specifying the spatial or temporal correlation. For practical engineering applications, current (and future) computational limitations demand that $\mathcal{M}$ describe turbulent as well as molecular transport. For example, in the simplest of these mixing models (Dopazo 1994),

$$\mathcal{M}\boldsymbol{\psi}^{(i)} = -\frac{\boldsymbol{\psi}^{(i)} - \frac{1}{N_p}\sum_{i=1}^{N_p}\boldsymbol{\psi}^{(i)}}{T_{\mathrm{mix}}},$$

where T_{mix} is an effective mixing time scale accounting for the enhanced diffusion due to turbulence. In application with RANS, T_{mix} is given by the integral timescale of the turbulence; with LES, by the micro-timescale.

In practice, (1.1) is usually integrated using a "time-splitting" method (Pope 1985): To calculate the change in $\boldsymbol{\psi}^{(i)}$ over a Δt, the $\mathcal{M}$ and $\mathcal{S}$ operations are applied separately, and each repeatedly in inverse proportion to the inherent time scales associated with each operator. For example, if the smallest chemical time scale is much smaller than the mixing time scale, the majority of the computational overhead will then be spent repetitively applying the $\mathcal{S}$ operator, *i.e.*, integrating

$$\frac{d}{dt}\boldsymbol{\psi}^{(i)}(t) = \mathcal{S}\boldsymbol{\psi}^{(i)}. \tag{1.2}$$

In practical applications, (1.2) is "stiff", that is, a large difference between the maximum and minimum absolute eigenvalues of the Jacobian of $\mathcal{S}$ exists. Physically, this is due to a large separation of the chemical time scales. Denote the chemical time scales by

$T_{\rm chem}$. Typically, in engineering applications, the minimum $T_{\rm chem} \sim 10^{-9}$ sec as compared to $T_{\rm mix} \sim 10^{-3}$ to 10^{-4} sec (Pope 1997) and hence most of the computational costs are spent integrating (1.2). Sophisticated software packages are generally available to integrate large systems of stiff equations (Byrne & Hindmarsh 1987). Due to the Jacobian evaluations, the computational time and storage requirements in solving (1.2) scale with N_s^2, seriously debilitating this approach for practical engineering applications where N_s is usually large. Parallelization of (1.2) is non-trivial.

Alternatively, a stochastic algorithm has been developed by Bunker *et al.* (1974) and Gillespie (1992) to solve (1.2). Briefly, the stochastic algorithm interprets the chemical reactions as random queuing events. The occurrence of a single reaction event follows a Poisson process, whose time scale depends upon the local state of the system. Thus, changes in "$\boldsymbol{\psi}^{(i)}$" do not occur over a fixed Δt, but follow from

$$\Delta t = \min\{(\Delta t)_1, (\Delta t)_2, \ldots, (\Delta t)_{N_r}, \} \tag{1.3}$$

where Δt is now a random variable defined by the set of exponentially distributed $(\Delta t)_k$, which describes the next time-of-arrival of the k-th reaction among the total number of reactions, N_r. Note that k and Δt are not independent random variables due to the min function of (1.3). With the arrival of each reaction event, the relevant species "concentrations" are updated accordingly. Note that, Jacobian evaluations are not required and, on average, the algorithm will automatically update changes in the faster species more often. The algorithm actually updates extrinsic values; the (intrinsic) concentrations are defined according to a system size (van Kampen 1992; Gardiner 1983). A review and formulation of the chemical Master equation by Poisson processes is described in Gardiner (1983). The computational time of the stochastic algorithm at an accuracy fixed by a number of realizations and/or number of stochastic particles will scale linearly with N_r. Storage requirements scale only linearly with N_s. These attributes make it ideal for systems with a large number of species. Parallelization of the algorithm is trivial, allowing essentially arbitrary tolerances (with unlimited processor number).

For the same computational time under serial computation, the stochastic algorithm yields less accurate solutions as compared to the deterministic approach or direct integration of (1.2). However, Bunker *et al.* (1974) report that, with acceptable statistical errors, the computational gain using the stochastic chemistry algorithm is a factor of 10 faster than direct integration. A reduced chemistry mechanism with $N_s = 6$ was used. Extrapolating to larger chemical kinetic mechanisms, a 10-fold increase in the number of species would result in a 10^2-fold increase in the computational time for direct integration and thus a total of a 100-fold gain in computational speed for the stochastic algorithm over direct integration assuming a 10-fold increase in the number of reactions.

The current state-of-the-art of the stochastic chemistry algorithm includes only zero-dimensional applications, *e.g.*, well-stirred reactor calculations, but apply realistic, Arrhenius and multi-step kinetic models. No transport model with the stochastic chemistry algorithm exists, motivating the present work. Following (1.3), the most straightforward method of introducing transport is through additional queuing events. In this paper, this is done by incorporating random walks and/or triplet maps into the algorithm. Representation of continuous laminar diffusive systems by stochastic methods (*i.e.*, jump process approximations for molecular diffusion and chemical reaction) are well-known, but limited to simple reaction (Gardiner 1983). Here, realistic, Arrhenius kinetics are also considered as well as turbulent transport.

At present, the main issues remaining in transported PDF modeling of turbulent premixed and nonpremixed combustion include:

(i) Accounting for the small-scale structure of turbulence in the micro-mixing models,
(ii) extension to the flamelet combustion regimes (another modeling issue), and
(iii) computational feasibility (predominantly an implementation issue).

The objectives of the paper are to address the latter two issues for applications to turbulent premixed combustion. Modeling approaches with regard to issue (i) usually employ stochastic methods to describe intermittency effects (Pope & Chen 1990; Fox 1997). With regard to issue (ii), Cha & Trouillet (2002*a*,*b*) have extended transported PDF modeling to the flamelet regime for nonpremixed combustion; no significant additional computational demands are required in correcting the reactive scalar timescales for many existing micro-mixing models. For the premixed case, Pope & Anand (1984) have treated flamelet combustion, but only in Damköhler's large-scale turbulence limit. Their method preserves the unmodified convective-diffusive flame structure of the preheat zone and is thus limited to the corrugated flamelet regime. Extension of their method to Damköhler's small-scale limit is described in this paper; again, no significant additional computational demands would be required over that of their existing approach of describing the corrugated flamelet regime. The present formulation of a transported PDF model for turbulent premixed combustion is applicable in both flamelet regimes and for distributed combustion (and the entire transition in between) with one unifying transport model: Kerstein's one-dimensional turbulence. Applications of Kerstein's one-dimensional turbulence concept to premixed flames using direct integration for the chemistry have been performed by Menon and co-workers with Fickian molecular diffusion replaced by a laminar flame propagation process (Menon & Kerstein 1992) and, more recently, by explicit finite differencing of the diffusion term (Smith & Menon 1996). Here, the one-dimensional turbulence concept with stochastic chemistry is developed.

The paper is organized as follows. In the next section, the canonical problem of a reaction-diffusion wave is described and the regimes of turbulent premixed combustion reviewed. Section 3 presents the results from two validation studies: (i) in the laminar case, one-dimensional premixed flames are simulated and their laminar flame speeds compared to exact solutions; and (ii) for an isotropic turbulence case, the scaling of the turbulent burning velocity is compared with the well-known relations in Damköhler's small- and large-scale turbulence limits. Conclusions are given in the final section.

2. Background

2.1. *The laminar premixed flame*

The simplest model, still preserving the underlying physics (enhanced transport due to chemical reaction, in this case), can be written as

$$\frac{\partial \Theta}{\partial t} = s\frac{\partial \Theta}{\partial z} + \mathcal{D}\frac{\partial^2 \Theta}{\partial z^2} + \dot{S} \tag{2.1}$$

for travelling wave solutions. Here, s is the propagation velocity (defined below), which is generally time-dependent, and $\dot{S}$ is the nonlinear source term of Θ. A transformation into a co-moving reference frame, $z \equiv x - st$, has been made from the laboratory reference frame, x, assuming waves travelling left to right. For a flame, this equation describes the transport of Θ from a "burnt" temperature $\Theta = \Theta_b$, $\dot{S} = 0$ at one boundary ($x = -\infty$) into the "unburnt" temperature $\Theta = \Theta_u$, $\dot{S} = 0$ at the other boundary ($x = +\infty$) with

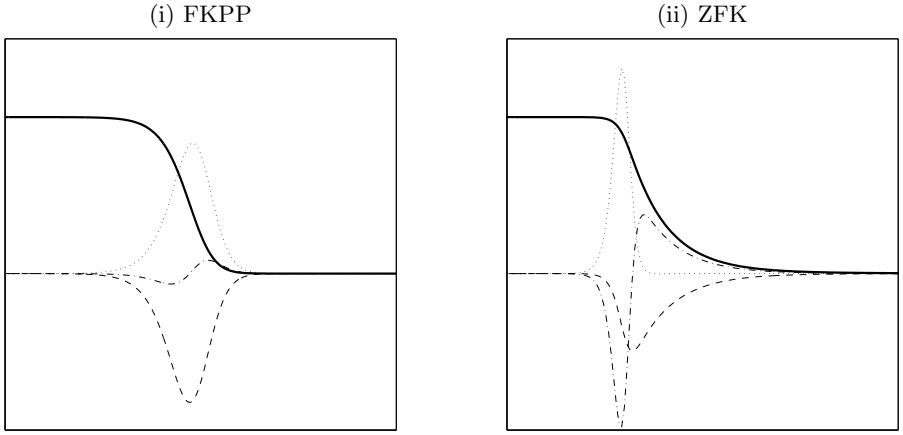

FIGURE 1. Structure of a one-dimensional laminar reaction-diffusion wave. Bold solid lines show the wave which travels left to right. Dash-dash lines are the convection term, dash-dot diffusion, and dot-dot the source term. Subplot (i) shows the structure of the Fisher (1937) and Kolmogorov *et al.* (1937) flame (FKPP); subplot (ii) the structure of the Zeldovich & Frank-Kamenetsky (1938) flame (ZFK).

$\Theta_u \leq \Theta \leq \Theta_b$, $\Theta > 0$. Two nonlinear source terms are considered based on the logistic form of $\dot{S} = k(\Theta - \Theta_u)(\Theta_b - \Theta)/(\Theta_b - \Theta_u)^2$ for (i) constant $k = A$ and (ii) for the Arrhenius formula$k = A\exp(-\Theta_a/\Theta)$ with large activation temperatures, $\Theta_a >> \Theta_b$, and constant A. The former source term is well-known in the natural sciences since its formulation by Fisher (1937) to describe a limiting case for the propagation of advantageous genes in a population; the latter, in combustion science following the pioneering work of Zeldovich & Frank-Kamenetsky (1938). See Williams (1985) and Clavin (1994) for details.

No known general analytical solution exists for the Zeldovich & Frank-Kamenetsky case, henceforth referred to as "ZFK" for convenience. Asymptotics (for large Θ_a) is described in Williams (1985) and Clavin (1994); clever iterative numerical strategies in Williams (1985). For the Fisher equation, the approximate analytical solution is due to Kolmogorov *et al.* (1937). We henceforth refer to this case as "FKPP". For both cases, the approximate solutions initialize finite-differenced numerical computations to yield their steady-state profiles. The Monte Carlo simulations (with the stochastic chemistry algorithm) are compared to these solutions (in section 3).

Defining $\theta \equiv (\Theta - \Theta_u)/(\Theta_b - \Theta_u)$ and the relevant length and time scales of the premixed flame as ℓ_F and T_F, respectively, yields the following nondimensionalized equations

$$\text{FKPP:}\quad 0 = \mu\frac{d\theta}{d\xi} + \frac{d^2\theta}{d\xi^2} + T_F A\theta(1-\theta) \tag{2.2a}$$

$$\text{ZFK:}\quad 0 = \mu\frac{d\theta}{d\xi} + \frac{d^2\theta}{d\xi^2} + T_F A\exp\left[-\frac{\text{Ze}(1-\theta)}{1-\alpha(1-\theta)}\right]\frac{\theta(1-\theta)}{1-\alpha(1-\theta)} \tag{2.2b}$$

where space has been nondimensionalized by ℓ_F (*e.g.*, $\xi \equiv z/\ell_F$) and time by T_F. With hindsight (Williams 1985; Clavin 1994; Kolmogorov *et al.* 1937), for $T_F A = 1/4$ in (2.2*a*), $\mu = 1$ and for $T_F A = \text{Ze}^2/2$ in (2.2*b*), $\mu = 1 - \mathcal{O}(1/\text{Ze})$ with $\text{Ze} >> 1$ and $\alpha \approx 1$. Here, $\alpha \equiv 1 - \Theta_u/\Theta_b$ is the heat-release parameter and $\text{Ze} \equiv \alpha\Theta_a/\Theta_b$ is the Zeldovich number

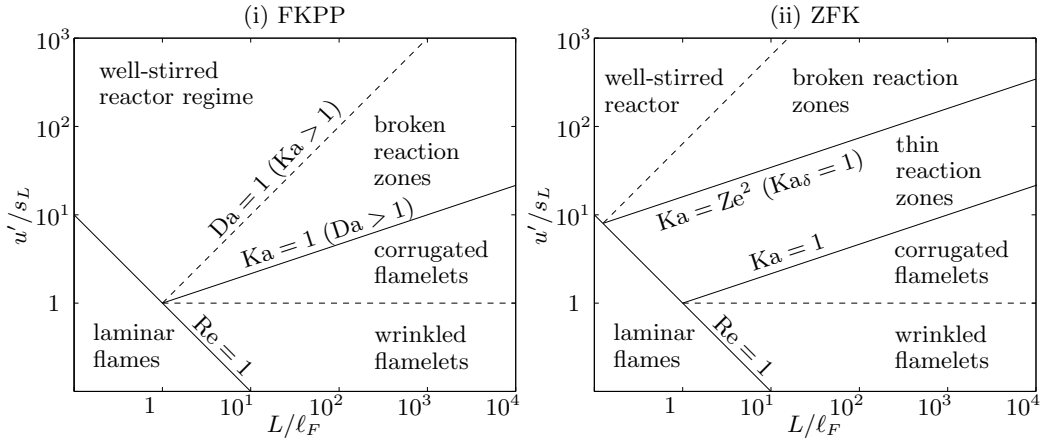

FIGURE 2. Turbulent premixed flame regime diagram (Bray & Peters 1994; Peters 2000) showing isolines of the various nondimensional numbers: $u'/s_L = \mathrm{Re}\ (L/\ell_F)^{-1}$, $u'/s_L = \mathrm{Da}^{-1}(L/\ell_F)$, and $u'/s_L = \mathrm{Ka}^{2/3}(L/\ell_F)^{1/3} = \mathrm{Ze}^{4/3}\mathrm{Ka}_\delta^{2/3}(L/\ell_F)^{1/3}$. Of course, with respect to the definitions of the Re and Da (and $\mathrm{Ka} = \mathrm{Ze}^2\mathrm{Ka}_\delta = \mathrm{Re}^{1/2}\mathrm{Da}^{-1}$), the regimes must be identical for the two cases. However, physical and semantic differences are to be distinguished for $\mathrm{Ka} > 1$ (Damköhler's small-scale turbulence limit) between the two cases. For the ZFK case, the additional regime of thin reaction zones (Peters 1999) is also a flamelet regime for the present one-step chemistry case (see discussion in section 3.2.)

(Williams 1985). In dimensional units, $s = \ell_F/T_F \equiv s_L$ (for the laminar case) are

$$\text{FKPP:}\quad s_L \approx \sqrt{\mathcal{D}\frac{A}{1/4}} \qquad \text{and} \qquad \text{ZFK:}\quad s_L \approx \sqrt{\mathcal{D}\frac{A}{\mathrm{Ze}^2/2}} \tag{2.3}$$

for the FKPP and ZFK cases, respectively.

Figure 1 shows the laminar flame structure for the FKPP and ZFK solutions. In subplot (ii), and in all subsequent calculations throughout the paper, $\alpha = 0.85$ and $\mathrm{Ze} = 8$. As is well known, for the ZFK case the large $\mathrm{Ze} >> 1$ confines the chemical source term to an inner reactive-diffusive zone of width $\ell_\delta \sim \mathcal{O}(\ell_F/\mathrm{Ze})$, resulting in a convective-diffusive balance within the outer zone (of thickness ℓ_F). For the FKPP case, a single convective-reactive zone dominates the entire flame thickness, as seen in figure 1 (i).

2.2. *The turbulent premixed flame*

Figure 2 reviews the various regimes of turbulent premixed combustion (Bray & Peters 1994; Peters 2000). We ignore the "well-stirred reactor" regime in both cases, as simple models already exist for this regime. Recall the definitions

$$\mathrm{Re}\ \mathrm{Sc} \equiv \frac{u'L}{\mathcal{D}} \qquad \text{and} \qquad \mathrm{Da} \equiv \frac{L/u'}{T_F}$$

which delineate the various regimes of turbulent premixed combustion. Here, u' is the turbulent velocity scale. Note that a single Damköhler number can be defined irrespective of the complexity of the chemistry (multiple chemistry times) by using the flame time. Unity Schmidt number is assumed ($\mathrm{Sc} = 1$). The so-called "wrinkled flamelets" regime, where $u' < s_L$, is also ignored. The remaining regimes then include the "thin reaction zones" (Peters 1999), broken reaction zones (formerly "distributed reaction zones" (Bray & Peters 1994)) and "corrugated flamelet" regimes which are divided by the unity Karlovitz

number line. Recall the definition of the Karlovitz number, $\mathrm{Ka} \equiv T_F/T_\eta$, where T_η is Kolmogorov's inner turbulence time scale. Following Peters (1999), for the ZFK case, the zone between $1 \leq \mathrm{Ka} \leq \mathrm{Ze}^2$ defines the regime of thin reaction zones. For the FKPP case and $\mathrm{Ka} > 1$, the broken reaction zones regime is a distributed combustion regime. For either the ZFK or FKPP case, $\mathrm{Ka} < 1$ is referred to as the corrugated flamelets regime (see figure 2).

The Karlovitz number is important as it distinguishes the scaling in Damköhler's small- and large-scale turbulence limits for another set of validation studies which predict the s_t/u' scaling with Da. Recall that, in Damköhler's small-scale turbulence limit, $\eta < \ell_F$ ($T_\eta < T_F$ or $\mathrm{Ka} > 1$) and the small-scale turbulence will modify the laminar flame structure. Employing an eddy diffusivity argument, $s_t \sim \sqrt{\mathcal{D}_t A}$ which follows from (2.3) with constant $\mathcal{D}_t$ or by dimensional analysis. Thus, it readily follows, with $\mathrm{Re} = \mathcal{D}_t/\mathcal{D}$, that

$$\frac{s_t}{u'} \sim \mathrm{Da}^{1/2}. \tag{2.4a}$$

This scaling is expected to be valid for the ZFK case (assuming the Kolmogorov eddies to be larger than $\ell_\delta \equiv \ell_F/\mathrm{Ze}$, the diffusive-reactive zone thickness). This is because eddy diffusivity successfully describes transport when convective-diffusive processes dominate. However, the scaling is questionable for the FKPP case as the leading-order solution, with or without all higher-order corrections, reveal an ever dominating convective-reactive balance.

In Damköhler's large-scale turbulence limit, $\eta > \ell_F$ ($T_\eta > T_F$ or $\mathrm{Ka} < 1$) and the laminar flame structure is preserved on average by definition. Due to this separation of the laminar flame and turbulence scales, the enhanced transport will be dominated by turbulence rather than reaction. This is because enhanced transport by turbulence is generally much more effective than enhanced transport due to chemical reaction and diffusion. A purely "kinematic scaling" is thus expected with s_t/u' then independent of Da (more precisely, the unmodified characteristic flame time):

$$s_t \sim u'. \tag{2.4b}$$

Recall that the BML model (Bray & Libby 1994) is strictly valid in Damköhler's (very) large-scale turbulence limit only: It follows that for $\eta >> \ell_F$, the details in the laminar flame structure are unimportant and a composite delta function PDF representation of the premixed flame would be sufficient.

3. Results and discussion

3.1. *Laminar premixed flame*

As a queuing process, incorporating Fickian diffusion by random walks in (2.1) is a straightforward extension of the stochastic chemistry algorithm. For simplicity, assume a uniformly-discretized grid of spacing Δx. Define the random variable Δt on the lhs of (1.3) as $(\Delta t)_{\mathrm{chem}}$, the random time increment to the next reaction event. Then, the time increment to the next reaction or diffusion event is given by the random variable

$$\Delta t = \min\{(\Delta t)_{\mathrm{diff}}, (\Delta t)_{\mathrm{chem}}.\} \tag{3.1}$$

With $T_{\mathrm{diff}} \equiv (\Delta x)^2/\mathcal{D}/2$ taken to be a deterministic time-of-arrival of a random walk (Feller 1970), $(\Delta t)_{\mathrm{diff}}$ is the remaining time to the next random displacement event. For the uniform grid spacing and a given $\mathcal{D}$, T_{diff} is independent of x. Thus, random walks are

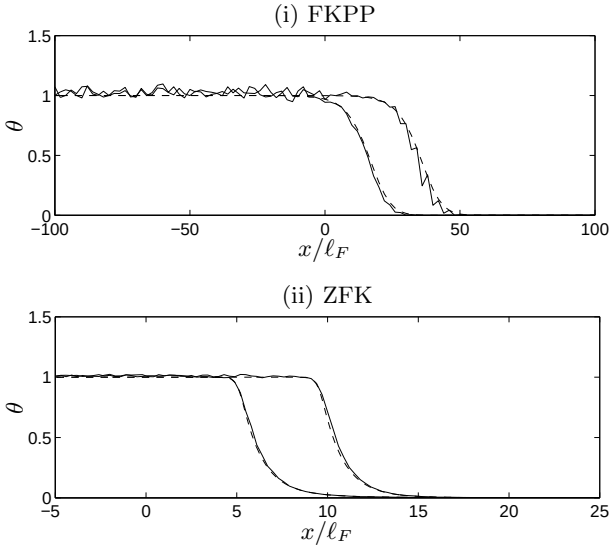

FIGURE 3. Typical realizations from the Monte Carlo simulations of the laminar FKPP and ZFK premixed flames. Solid lines are the simulation results. For the (i) FKPP case, the two solutions are between 20 nondimensional time units t/T_F with dash-dash lines from deterministic, finite-differenced solutions. For the (ii) ZFK case, between 5 nondimensional time units with dash-dash lines from finite-differenced solutions.

applied at every grid point every T_{diff}. Update of the species populations follow the jump process as described by the stochastic chemistry algorithm at every grid point. Values of the species populations can be converted to and from concentrations *via* van Kampen's system size. For example, the initial (intrinsic) concentration, $\theta(x)$, are converted to extrinsic (integer) values, M, for every subvolume, Δx, following $M = \text{round}\{\Omega \times \theta\}$, where $\Omega = n_p \Delta x$ and $n_p(x)$ is the number of particles in a cell. Sensitivity to the system size, or n_p for fixed Δx, is described below.

Figure 3 compares the Monte Carlo simulation results to the exact and approximate flame solutions for the FKPP and ZFK cases, respectively. Qualitatively, the Monte Carlo simulations are in good agreement with the deterministic solutions for the flame structure. Defining a single realization as a simulation with duration of approximately 10 T_F, a quantitative assessment can be made using flame-speed calculations.

For numerical simulations of a reaction-diffusion wave (Monte Carlo or otherwise), a practical measure of the flame speed is first required. One can be derived by integrating the governing equations in lab coordinates from a reference position in the burnt region, x_b say. Leibniz's rule gives $\frac{d}{dt}\int_{x_b}^{\infty} \Theta dx + \frac{dx_b}{dt}\Theta_b = \int_{x_b}^{\infty} \dot{S} dx$, where x_b is sufficiently upstream from the flame that $(d\Theta/dx)_{x_b} = 0$ holds. Since $s = \int \dot{S} dx$, it follows that

$$s = \frac{d}{dt}\int_{x_b}^{\infty} \Theta dx \tag{3.2}$$

for a fixed x_b. Thus, $s(t)$ can be estimated by the local time derivative of $\int \Theta dx \equiv H(t)$. At "steady-state", characterized by a constant wave speed, $H(t)$ will be linear and s given by its slope. Note, this is valid for calculating the flame speed for both the laminar case ($s = s_L$) and the flame speed for a turbulent Θ field ($s \to s_t$) along the mean direction of propagation, also denoted by x. For the latter case, although pedagogically misleading, we refer to s_t as a "turbulent flame speed". (The definition of s_t and its distinction from s for the turbulent case is described later in section 3.2.)

For Monte Carlo simulations, convergence of the statistical errors from the flame speed

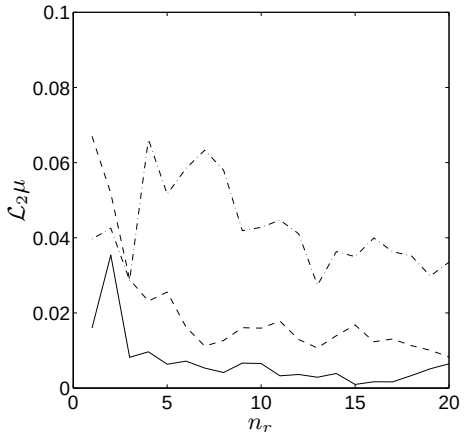

FIGURE 4. Monte Carlo statistical errors with the number of realizations, n_r, for the laminar flame speed calculated from (3.2). The figure shows three sets of calculations: $n_p = 10^3$ (dash-dot line), 10^4 (dash-dash), and 10^5 (solid line). The FKPP case is shown. Results for the ZFK case are comparable.

calculation procedure can be gauged using the $\mathcal{L}_2$ error estimator

$$\mathcal{L}_2\mu \equiv \left[\left(\frac{1}{n_r}\sum_{k=1}^{n_r}\mu^{(k)} - 1\right)^2\right]^{1/2},$$

where $\mathcal{L}_2\mu$ is a function of n_r, the number of realizations, and $\mu^{(k)} \equiv s^{(k)}\ T_F/\ell_F$ is the nondimensional flame speed for the k-th realization calculated using (3.2).

Figure 4 shows the convergence of the statistical errors with n_p (with Δx fixed) and n_r for the laminar flame-speed calculation procedure. For a fixed and sufficiently large n_r, the figure just shows the well-known $1/n_p^{1/2}$ scaling of the Monte Carlo statistical errors. For a fixed system size, the figure shows that the flame-speed calculation procedure requires only a few realizations to reach the asymptotic error at $n_r >> 1$. The figure can be interpreted as follows: The flame-speed calculation procedure yields less than, for example, a 5% error using $n_p \sim 10^3$ and $n_r \gtrsim 10$, or $n_p \sim 10^4$ and $n_r \gtrsim 1$, etc.

3.2. *Turbulent premixed flame*

Kerstein's linear-eddy variant (Kerstein 1991*a*,*b*) of his one-dimensional turbulence concept is incorporated with the stochastic chemistry and mixing algorithm of section 3.1. This is straightforward as the advective stirring processes are already represented by a queuing process through the triplet mapping procedure. Define the Poisson random variable $(\Delta t)_{\rm stir}$ as the next time-of-arrival of each eddy or mapping event. Then, the time increment to the next reaction, molecular diffusion, or advective stirring event is given by the random variable

$$\Delta t = \min\{(\Delta t)_{\rm stir}, (\Delta t)_{\rm diff}, (\Delta t)_{\rm chem}\}, \tag{3.3a}$$

where $(\Delta t)_{\rm diff}$ and $(\Delta t)_{\rm chem}$ have been defined with regard to (3.1).

The resulting one-dimensional turbulent premixed flame model is an abstraction. However, the expected qualitative features of the turbulence-chemistry interaction are reproduced by the Monte Carlo simulations. Figure 5 shows typical realizations of the flame structure in Damköhler's small- and large-scale turbulence limits in subplots (i) and (ii), respectively, for the FKPP reaction-diffusion wave. Single realizations are shown by the solid lines; the ensemble average summed over 10^2 realizations at the same time are shown by the dash-dash lines. In both subplots, Re = 100. In subplot (i), Da = 5, and in

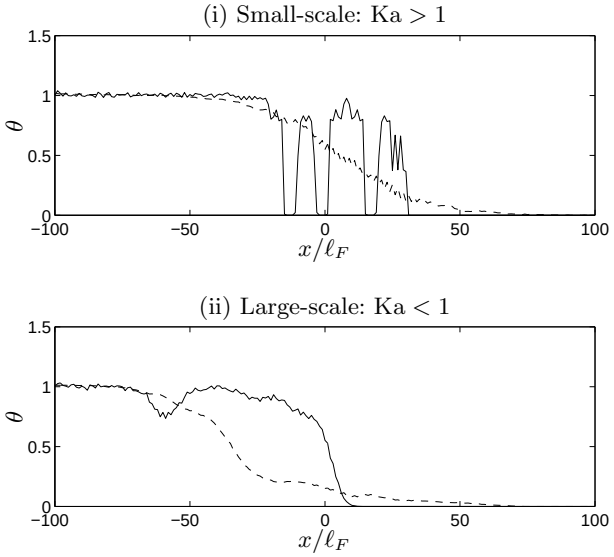

FIGURE 5. Typical realizations from the Monte Carlo simulations of the turbulent FKPP premixed flame. Solid lines are the simulation results; dash-dash lines are ensemble averages of 10^2 realizations at the same time. Turbulent transport is modeled using Kerstein's linear eddies. The corresponding laminar results are shown in figure 3. In both figures, Re = 100. In subplot (i), Da = 5 (hence Ka = $\mathrm{Re}^{1/2}/\mathrm{Da}$ = 2); in subplot (ii), Da = 50 (hence Ka = 0.2).

subplot (ii), Da = 50. Thus, in subplot (i), Ka > 1 and the smallest turbulent eddies will modify the laminar flame structure since $\eta < \ell_F$. This is clearly observed in the single realizations (solid lines) of figure 5 (i). Figure 3 (i) shows the corresponding laminar case. In figure 5 (ii), Ka < 1 and the turbulence does not modify the laminar flame structures. Preservation of the laminar flame scales is visibly apparent upon comparing the single realizations (solid lines) in figure 5 (ii) with the corresponding laminar case in Fig. 3 (i). The qualitative features of the turbulence-chemistry interaction for the ZFK case are similar.

The expected quantitative results for the "turbulent flame speed" are also reproduced by the stochastic model. Figure 6 shows the turbulent flame speed calculated using (3.2) over a range of Damköhler numbers, for the ZFK reaction-diffusion wave. Each point represents a single realization; big dots are the conditional (on Da) average. "s_t" is used to distinguish this average from the "s" of each realization from figure 3.2. The unity Karlovitz number line is demarcated by the bold dot-dot line. Subplot (i) shows on log-log scale the subset of realizations in subplot (ii) for which Ka > 1. For Ka > 1 ($\eta < \ell_F$), subplot (i) shows that the modeling predicts the expected s_t/u' dependence on Da as given by (2.4a) for Damköhler's small-scale turbulence limit. For Ka < 1 ($\eta > \ell_F$), s_t/u' becomes independent of Da for increasing Da, validating the model in Damköhler's large-scale turbulence limit as well.

We note in passing the increasing scatter of s with Da in figure 6. For a given Da bin size, the number of realizations are too large for the observed scatter to be solely due to statistical error. Following the analysis of the statistical errors for the flame-speed calculation procedure in the previous subsection, the statistical errors would only account for a small fraction of the scatter (even for a Da bin size which includes only 10 realizations). Physically, the increasing scatter in s/u' with Da is to be expected since, for fixed Re, the increasing range of turbulent length scales would create an increasing variation in the s "measurements" taken at the same time amongst an increasing number of realizations. Evidently, the intermittency effects on s, also observed in experimental data, are captured by the present modeling.

To introduce the less-computationally-expensive Taylor diffusion model into the sim-

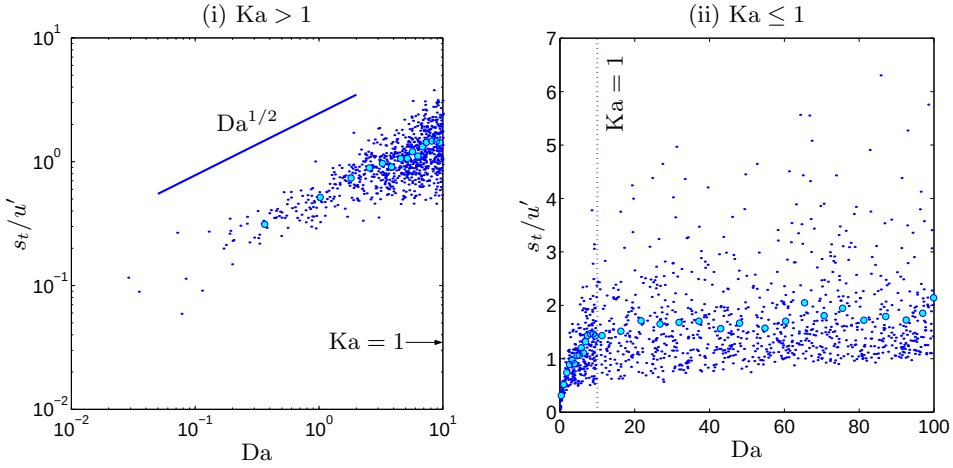

FIGURE 6. Scaling of s_t/u' with Da in Damköhler's small- (Ka > 1) and large-scale (Ka < 1) turbulence limits for the ZFK premixed flame. A subset of the same data in subplot (ii) is shown in subplot (i), which shows Damköhler's small-scale turbulence scaling of $s_t/u' \sim \mathrm{Da}^{1/2}$ for Ka > 1. Recall that Da Ka = $\mathrm{Re}^{1/2}$.

ulations in place of Kerstein's linear eddy model, consider the ZFK case in Damköhler's small-scale turbulence limit, whose scaling is given by (2.4*a*). Representing the classic engineering approach, the main motivating idea behind Taylor diffusion here is to reproduce the turbulent flame-speed scaling directly without performing multiple realizations for a fixed Da. This scaling is thus trivially reproduced by simulating a "laminar" flame but with the molecular diffusivity replaced by an "eddy diffusivity". In other words, instead of using (3.3*a*), turbulent and molecular transport can be simulated together following

$$\Delta t = \min\{(\Delta t)_{\mathrm{mix}}, (\Delta t)_{\mathrm{chem}}, \} \tag{3.3b}$$

which is analogous to (3.1) but with $\mathcal{D}$ in $(\Delta t)_{\mathrm{diff}}$ replaced by $\mathcal{D}_t = \mathrm{Re}\ \mathcal{D}$ for $(\Delta t)_{\mathrm{mix}}$. Equation (2.3) then gives the turbulence enhanced flame speed, s_t, and so the scaling given by (2.4*a*) is trivially reproduced (although without intermittency). It is interesting and useful to ask what is lost with the faster computations resulting from replacing T_{stir}, the range of turbulent timescales, and T_{diff} by T_{mix} alone (besides losing the true scatter in the turbulent flame-speed predictions)? It is argued that this question is equivalent only to asking: When is the regime of thin reaction zones a true flamelet regime? Consideration of the limitations of Taylor diffusion for the corrugated flamelet regime yields a simple transported PDF model for turbulent premixed combustion valid in both Damköhler's small- and large-scale turbulence limits.

For the regime of thin reaction zones, consider again the ZFK case with one-step chemistry. Recall that Taylor diffusion works when advective and diffusive processes are unmodified by reaction. That reaction does not directly impact the enhanced convective-diffusive transport in the modified preheat zone is guaranteed by the high activation temperature (Ze >> 1) of the reaction. This is because, with the one-step reaction, only temperatures between $(1 - 1/\mathrm{Ze}) < \theta < 1$, which have a low probability of occurance in the modified preheat zone under the defined restrictions, will lead to a non-negligible reaction rate. Thus, only convective-diffusive effects remain important outside the inner reactive-diffusive boundary layer. This is clear for the present one-step chemistry case. For multi-step chemistry, assume that T_{chem}, the range of chemistry timescales, and T_{diff}

yield a well defined flame time scale irrespective of the modified preheat zone. Taylor diffusion would thus be valid so long as the inner zone remains intact. The repercussions of this assumption being valid are significant. For example, consider the transported PDF model of Pope & Anand (1984), where the combined contributions from the diffusion and chemical source terms in the transported PDF equation for a reacting scalar, ψ say, are modeled together by a known function $h(\psi)$. In Damköhler's large-scale turbulence limit then, $h(\psi)$ is the response of the convection term of the steady planar laminar premixed flame and is known ahead of time for a given chemical kinetic scheme. Extension to the thin reaction zones regime can simply be done by parameterizing $h(\psi) \rightarrow h_t(\psi)$ by $\mathcal{D} \rightarrow \mathcal{D}_t$, where $h_t(\psi; \mathcal{D}_t)$ would be pretabulated in practice for an expected range of $\mathcal{D}_t$. It is no surprise that such a tabulation over a "parameter" governed by the large scales can be performed if the thin reaction zones regime is a flamelet regime.

In the corrugated flamelet regime, the less computationally-expensive algorithm represented by (3.3*b*) will obviously give the wrong scaling for the turbulent flame speed. This is of minor concern, as s_t/u' changes little with large Da due to the weak $\mathrm{Da}^{1/2}$ dependence in Damköhler's small-scale turbulence limit. (Of major concern would be the neglect of the increasing level of s fluctuations with Da.) Or, if this regime is of practical interest, and the transition between Damköhler's small- and large-scale turbulence limits can be neglected, the above tabulation procedure can readily be modified to yield a unique $h_t(\psi; \mathcal{D}_t) = h(\psi)$ for all values of $\mathcal{D}_t$ above a threshold value. (Of course, the effect of the largest fluctuations in s, which occur in the large-scale limit, would also have to be negligible as well.) Certainly, semi-empirical or purely empirical correlations for s_t/u' from a given application can also be used to pretabulate $h_t(\psi; \mathcal{D}_t)$ as well, since s_t can be related to $\mathcal{D}_t$. A semi-empirical correlation for s_t/u' has been developed and applied by Peters (1999) to convect a level-set surface representing the inner reaction zone. If intermittency effects must be accounted for, the present transported PDF model with Taylor diffusion becomes questionable as it incorrectly assumes that the turbulent flame speed (or turbulent diffusivity) is a well-defined, physical quantity.

4. Conclusions and future work

Currently, transported PDF methods of turbulent combustion discount the flame structures which can modify the unresolved mixing processes. Accounting for flamelet combustion in micro-mixing models for turbulent nonpremixed combustion is described in Cha & Trouillet (2002*a*,*b*). Here, for the premixed case, enhanced molecular transport due to reaction as well as turbulence must be accounted for. Pope & Anand (1984) have treated turbulent premixed combustion in the corrugated flamelet regime by a transported PDF method; here, their method is extended to the "thin reaction zones" regime (Peters 1999). In the thin reaction zones regime, the characteristic laminar flame scales are modified by the turbulence, but the inner layer reaction zone and turbulence scales remain separated due to a large activation energy. Neglecting intermittency effects, this allows the turbulence broadened preheat zone to be described by eddy diffusivity and hence the response of the flame structure to the turbulent mixing processes to be pretabulated for a given chemistry scheme in practice.

For distributed combustion, the interaction with the range of chemistry time scales must be accounted for and the issue of computational feasibility of transported PDF modeling arises if detailed kinetics are required. The stochastic chemistry algorithm of Bunker *et al.* (1974) and Gillespie (1992) is extended to treat transport to help off-

set the significant computational demands required for describing complex chemistry in transported PDF methods. Molecular and turbulent transport are integrated into the stochastic chemistry algorithm as queuing processes. For simplicity, a freely propagating premixed flame driven by a one-step chemical reaction is considered. Two nonlinear source terms, with and without high activation energy and referred to as the FKPP and ZFK cases, respectively, define two representative nonconservative systems for model investigation and validation (see (2.2) in this paper).

For the laminar cases, results from the Monte Carlo simulations are compared to exact deterministic, finite-differenced solutions and validate the approach for molecular transport and transport by eddy diffusivity. For the turbulent case, Kerstein's one-dimensional turbulence concept is used to incorporate the entire dynamic range of turbulent motions in the more general, but more computationally-expensive, model. (The model is general because it can be applied without *ad hoc* knowledge of the regime.) The resulting simulations are able to reproduce the expected scalings in Damköhler's small- and large-scale turbulence limits. Results, not presented here, also show good agreement with the experimental data sets of Abdel-Gayed & Bradley (1981) and Bradley *et al.* (1992). If intermittency effects can be neglected, Taylor diffusion represents a less physical, but less computationally-expensive model of turbulent transport. The ZFK case exemplifies an ideal scenario where the thin reaction zones regime is a flamelet regime on average and Taylor diffusion modeling of transport is valid. In contrast, distributed combustion occurs in the FKPP case when the smallest turbulent scales interact with the characteristic flame scale.

In immediate future work, the general algorithm represented by (3.3*a*) can be applied to study distributed combustion. Results for the FKPP case, not presented here, yield a counter-intuitive, reaction independent $s_t/u' \sim \mathrm{Da}^{1/2}$ scaling (as the Taylor diffusion model would yield by definition)! In other future work, the computational savings which result from using stochastic chemistry can be spent on multi-step chemistry and/or multi-dimensional simulations. For example, describing local sources/sinks by a queuing process offers a straightforward means of incorporating chemical reaction in cellular automata or lattice Boltzmann simulations.

REFERENCES

Abdel-Gayed, R. G. & Bradley, D. 1981 A two-eddy theory of premixed turbulent flame propagation. *Phil. Trans. Roy. Soc. Lond. A* **301**, 1–25.

Bradley, D., Lau, A. K. C. & Lawes, M. 1992 Flame stretch as a determinant of turbulent burning velocity. *Phil. Trans. Roy. Soc. Lond.* **338**, 359–387.

Bray, K. N. C. & Libby, P. A. 1994 Recent developments in the BML model of premixed turbulent combustion. In *Turbulent Reacting Flows*, chap. 3, pp. 115–151. Academic, New York.

Bray, K. N. C. & Peters, N. 1994 Laminar flamelets in turbulent flames. In *Turbulent Reacting Flows*, chap. 2, pp. 63–113. Academic, New York.

Bunker, D. L., Garrett, B., Kleindienst, T. & Iii, G. S. L. 1974 Discrete simulation methods in combustion kinetics. *Combust. Flame* **23**, 373–379.

Byrne, G. D. & Hindmarsh, A. C. 1987 Stiff ODE solvers: A review of current and coming attractions. *J. Comput. Phys.* **70**, 1–62.

Cha, C. M. & Trouillet, P. 2002*a* A model for the mixing time scale of a turbulent reacting scalar. *Phys. Fluids* (submitted).

Cha, C. M. & Trouillet, P. 2002*b* A subgrid mixing model for large-eddy simulations of turbulent reacting flows using the filtered density function. *Phys. Fluids* (submitted).

Clavin, P. 1994 Premixed combustion and gasdynamics. In *Annu. Rev. Fluid Mech.* bf 26, 321–352.

Dopazo, C. 1994 Recent developments in PDF methods. In *Turbulent Reacting Flows* (P. A. Libby & F. A. Williams, eds.), chap. 7, pp. 375–474. Academic, New York.

Feller, W. 1970 *An Introduction to Probability Theory and Its Applications*, 3rd edn. Wiley, New York.

Fisher, R. A. 1937 The wave advance of advantageous genes. *Ann. Eugenics* **7**, 355–369.

Fox, R. O. 1997 The Lagrangian spectral relaxation model of the scalar dissipation in homogeneous turbulence. *Phys. Fluids* **9** (8), 2364–2386.

Gardiner, C. W. 1983 *Handbook of Stochastic Methods for Physics, Chemistry and the Natural Sciences*. Springer New York.

Gillespie, D. T. 1992 *Markov Processes*. Academic, New York.

van Kampen, N. G. 1992 *Stochastic Processes in Physics and Chemistry*. Amsterdam: North-Holland.

Kerstein, A. R. 1991*a* Linear eddy model of turbulent scalar transport. Part 6: Microstructure of diffusive scalar mixing fields. *J. Fluid Mech.* **231**, 361.

Kerstein, A. R. 1991*b* Linear-eddy modeling of turbulent transport. Part V: Geometry of scalar interfaces. *Phys. Fluids A* **3**, 1110–1114.

Kolmogorov, A. N., Petrovsky, I. G. & Piscounov, N. S. 1937 Study of the diffusion equation with a source term and its application to a biological problem. *Bull. State Univ. Moscow* **1**, 1–25.

Menon, S. & Kerstein, A. R. 1992 Stochastic simulation of the structure and propagation rate of turbulent premixed flames. *Proc. Combust. Inst.* **24**, 443–450.

Peters, N. 1999 The turbulent burning velocity for large scale and small scale turbulence. *J. Fluid Mech.* **384**, 107–132.

Peters, N. 2000 *Turbulent Combustion*. Cambridge University Press.

Pope, S. B. 1985 PDF methods for turbulent reacting flows. *Prog. Energy Combust. Sci.* **11**, 119–192.

Pope, S. B. 1990 Computations of turbulent combustion: Progress and challenges. *Proc. Combust. Inst.* **23**, 591–612.

Pope, S. B. 1997 Computationally efficient implementation of combustion chemistry using *in situ* adaptive tabulation. *Combust. Theory Modelling* **1**, 41–63.

Pope, S. B. & Anand, M. S. 1984 Flamelet and distributed combustion in premixed turbulent flames. *Proc. Combust. Inst.* **20**, 403–410.

Pope, S. B. & Chen, Y. L. 1990 The velocity-dissipation pdf model for turbulent flows. *Phys. Fluids A* **2**, 1437.

Smith, T. & Menon, S. 1996 Model simulations of freely propagating turbulent premixed flames. *Proc. Combust. Inst.* **26**, 299–306.

Williams, F. A. 1985 *Combustion Theory*. Benjamin-Cummings, San Francisco..

Zeldovich, Y. B. & Frank-Kamenetsky, D. A. 1938 A theory of thermal propagation of flame. *Acta Physicochim. URSS* **9**, 341–350.